Origin and Properties of the Gap in the Half-Ferromagnetic Heusler Alloys

I. Galanakis* and P. H. Dederichs
Institut für Festkörperforschung, Forschungszentrum Jülich, D-52425 Jülich, Germany

N. Papanikolaou
Fachbereich Physik, Martin-Luther Universität, Halle-Wittenberg, D-06099 Halle, Germany

(Dated: February 1, 2008)

We study the origin of the gap and the role of chemical composition in the half-ferromagnetic Heusler alloys using the full-potential screened KKR method. In the paramagnetic phase the $C1_b$ compounds, like NiMnSb, present a gap. Systems with 18 valence electrons, Z_t, per unit cell, like CoTiSb, are semiconductors, but when $Z_t > 18$ antibonding states are also populated, thus the paramagnetic phase becomes unstable and the half-ferromagnetic one is stabilized. The minority occupied bands accommodate a total of nine electrons and the total magnetic moment per unit cell in μ_B is just the difference between Z_t and 2×9. While the substitution of the transition metal atoms may preserve the half-ferromagnetic character, substituting the *sp* atom results in a practically rigid shift of the bands and the loss of half-metallicity. Finally we show that expanding or contracting the lattice parameter by 2% preserves the minority-spin gap.

PACS numbers: 71.20.-b, 71.20.Be, 71.20.Lp

I. INTRODUCTION

Heusler alloys[1] have attracted during the last century a great interest due to the possibility to study in the same family of alloys a series of interesting diverse magnetic phenomena like itinerant and localized magnetism, antiferromagnetism, helimagnetism, Pauli paramagnetism or heavy-fermionic behavior.[2,3,4] The first Heusler alloys studied were crystallizing in the $L2_1$ structure which consists of 4 fcc sublattices. Afterwards, it was discovered that it is possible to substitute one of the four sublattices with vacancies ($C1_b$ structure). The latter compounds are often called half-Heusler alloys, while the $L2_1$ compounds are often referred to as full-Heusler alloys. In 1983 de Groot and his collaborators[5] showed that one of the half-Heusler compounds, NiMnSb, is a half-ferromagnet, i.e. the minority band is semiconducting with a gap at the Fermi level E_F, leading to 100% spin polarization at E_F. Recently the rapid development of magnetoelectronics intensified the interest on such materials. Adding the spin degree of freedom to the conventional electronic devices has several advantages like the nonvolatility, the increased data processing speed, the decreased electric power consumption and the increased integration densities.[6] The current advances in new materials are promising for engineering new spintronic devices in the near future.[6] Other known half-ferromagnetic materials are CrO_2,[7] $La_{0.7}Sr_{0.3}MnO_3$,[7] the diluted magnetic semiconductors[8] like (In,Mn)As and very recently also CrAs in the zinc-blende structure was proposed to be a half-ferromagnet.[9] Although thin films of CrO_2 and $La_{0.7}Sr_{0.3}MnO_3$ have been verified to present practically 100% spin-polarization at the Fermi level at low temperatures,[7,10] NiMnSb remains attractive for technical applications like spin-injection devices,[11] spin-filters,[12] tunnel junctions,[13] or GMR devices[14] due to its relatively high Curie temperature ($T_c \simeq$730K) compared to these compounds.[2]

The half-ferromagnetic character of NiMnSb in single crystals has been well-established experimentally. Infrared absorption[15] and spin-polarized positron-annihilation[16] gave a spin-polarization of ∼100% at the Fermi level. Recently high quality films of NiMnSb have been grown,[17] but they were found not to reproduce the half-ferromagnetic character of the bulk. Values of 58% and 50% for the spin-polarization at the Fermi level were obtained by Soulen *et al.*[7] and by Mancoff *et al.*,[18] respectively, and recently Zhu *et al.*[19] found a value of 40% using spin-resolved photoemission measurements on polycrystalline films. Ristoiu *et al.*[20] showed that during the growth of the NiMnSb thin films, Sb atoms segregate to the surface decreasing the obtained spin-polarization; they measured a value of ∼30% at 200K, while at room temperature the net polarization was practically zero. But when they removed the excess of Sb by a flash annealing, they managed to get a nearly stoichiometric ordered alloy surface terminating in MnSb. Inverse photoemission experiments at room temperature revealed that the latter surface shows a spin-polarization of about 67±9% which is significantly higher than all previous values.[20] Finally there is experimental evidence that for a temperature of ∼80 K there is transition from a half metal to a normal ferromagnet,[21] but these experiments are not yet conclusive.

Several groups have verified the half-ferromagnetic character of bulk NiMnSb using first-principles calculations[22,23] and its magnetic properties can be well-understood in terms of the hybridization between the higher-valent 3*d* atom (like Ni) and Mn, and the indirect exchange of the Mn *d* electrons through the *sp* atom.[24,25] Larson *et al.* have shown that the actual structure of NiMnSb is the most stable with respect to an interchange of the atoms[26] and Orgassa *et al.* showed that a few percent of disorder induce states

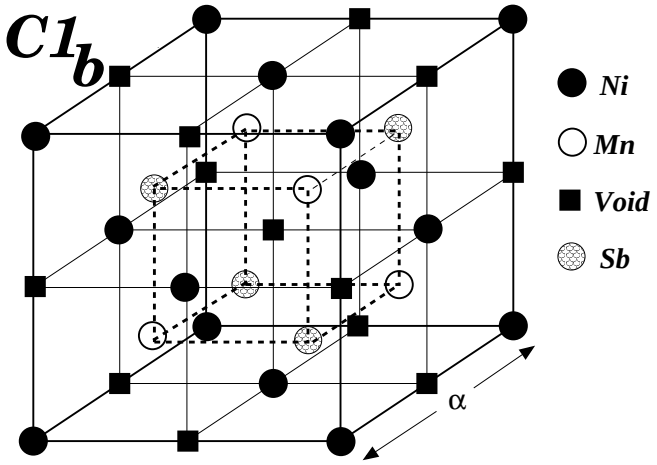

FIG. 1: Schematic representation of the $C1_b$ structure. The lattice consists of 4 fcc sublattices. The unit cell is that of a fcc lattice with four atoms as basis: Ni at (0 0 0), Mn at $(\frac{1}{4}\ \frac{1}{4}\ \frac{1}{4})$, a vacant site at $(\frac{1}{2}\ \frac{1}{2}\ \frac{1}{2})$ and Sb at $(\frac{3}{4}\ \frac{3}{4}\ \frac{3}{4})$ in Wyckoff coordinates

within the gap but do not destroy the half-metallicity.[27] Ab-initio calculations[28,29] have shown that the NiMnSb surfaces do not present 100% spin-polarization at the Fermi level and it was proposed by Wijs and de Groot that at some interfaces it is possible to restore the half-ferromagnetic character of NiMnSb.[28] Jenkins and King[30] using a pseudopotential technique showed that the MnSb terminated (001) NiMnSb surface relaxes mildly; the Sb atoms move slightly outwards and the Mn inwards with a total buckling of only 0.06 Å. They identified two surface states in the minority band inside the gap, which cross the Fermi level and which are strongly localized in the surface region.

In this contribution we will study the origin of the gap and different ways to influence the position of the Fermi level that can lead to new half-ferromagnetic Heusler materials which might have advantages as compared to the NiMnSb films and therefore could be more attractive for applications. In Section II we present the details of our calculations and in Section III we discuss the properties of the XMnSb compounds, where X stands for Ni, Co, Rh, Pd, Ir or Pt. In Section IV we study the influence of the lattice parameter on the position of the Fermi level and in Section V we investigate the origin of the gap. In Sections VI and VII we study the influence of the lower-valent transition metal and of the *sp* atom, respectively, on the properties of the gap. Finally in Section VIII we conclude and summarize our results.

II. COMPUTATIONAL DETAILS

To perform the calculations, we used the Vosko, Wilk and Nusair parameterization[31] for the local density approximation (LDA) to the exchange-correlation potential[32] to solve the Kohn-Sham equations within the full-potential screened Korringa-Kohn-Rostoker (FKKR) method.[33,34] The full-potential is implemented by using a Voronoi construction of Wigner-Seitz polyhedra that fill the space as described in Ref. 34. A repulsive muffin-tin potential (4 Ry high) is used as reference system to screen the free-space long-range structure constants into exponentially decaying ones.[35] For the screening we took for all compounds interactions up to the sixth neighbors into account leading to a tight-binding (TB) cluster around each atom of 65 neighbors. To calculate the charge density, we integrated along a contour on the complex energy plane, which extends from the bottom of the band up to the Fermi level.[36] Due to the smooth behavior of the Green's functions for complex energies, only few energy points are needed; in our calculations we used 42 energy points. For the Brillouin zone (BZ) integration, special points are used as proposed by Monkhorst and Pack.[37] Only few tens of **k** are needed to sample the BZ for the complex energies, except for the energies close to the real axis near the Fermi level for which a considerably larger number of **k**-points is needed. We have used a 30×30×30 **k**-space grid in the full BZ to perform the integrations. In addition we used a cut off of ℓ_{max}=6 for the multipole expansion of the charge density and the potential and a cut off of ℓ_{max}=3 for the wavefuctions. Finally in our calculations the core electrons are allowed to relax during the self-consistency.

In Fig. 1 we show the $C1_b$ structure, which consists of four fcc sublattices. The unit cell is that of a fcc lattice with four atoms as basis at A=(0 0 0), B=$(\frac{1}{4}\ \frac{1}{4}\ \frac{1}{4})$, C=$(\frac{1}{2}\ \frac{1}{2}\ \frac{1}{2})$ and D=$(\frac{3}{4}\ \frac{3}{4}\ \frac{3}{4})$ in Wyckoff coordinates. In the case of NiMnSb the A site is occupied by Ni, the B site by Mn and the D site by Sb, while the C site is unoccupied. The $C1_b$ structure is similar to the $L2_1$ structure adopted by the full Heusler alloys, like Ni_2MnSb where also the C site is occupied by a Ni atom. We should also mention that the zinc-blende structure adopted by a large number of semiconductors, like GaAs, ZnSe, InAs etc., is also consisting of four fcc sublattices. In the case of GaAs the A site is occupied by a Ga atom, the B site by a As atom, while the C and D sites are empty. This close structure similarity makes the Heusler alloys compatible with the existing semiconductor technology and thus very attractive for industrial applications.

III. X-MnSb COMPOUNDS WITH X= Co, Ni, Rh, Ir, Pd AND Pt

Firstly we calculated the electronic structure of the XMnSb, with X being an element of the Co or Ni columns in the periodic table. We used as lattice parameters the experimental ones for all compounds.[2] These compounds are known experimentally to be ferromagnets with high Curie temperatures ranging between 500 K and 700 K for the Co, Ni, Pd and Pt compounds, while the Curie temperatures of the Ir and Rh compounds are around room temperature.[2] We should also men-

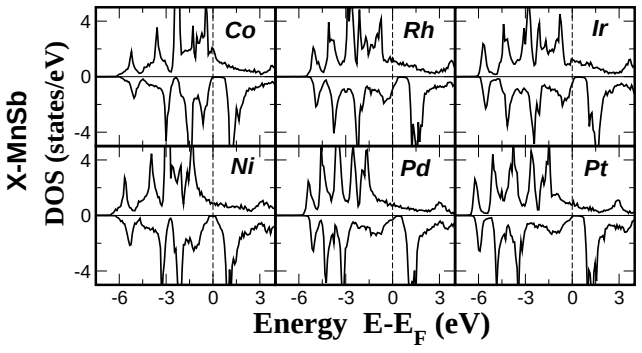

FIG. 2: Spin-projected density of states for the XMnSb Heusler alloys. They all posses a spin-down gap but only in Co-, Ni- and Pt- based ones is the Fermi level (zero at the energy axis) inside the gap.

TABLE I: Spin magnetic moments in μ_B using the experimental lattice constants (see Ref. 2) except for FeMnSb where we have used the lattice parameter estimated in Ref. 43. They are calculated by integrating the spin-projected charge density inside the Wigner-Seitz polyhedron containing the atom. X stands for the atom occupying the A site (see Fig. 1).

$m^{\rm spin}(\mu_B)$	X	Mn	Sb	Void	Total
NiMnSb	0.264	3.705	-0.060	0.052	3.960
PdMnSb	0.080	4.010	-0.110	0.037	4.017
PtMnSb	0.092	3.889	-0.081	0.039	3.938
CoMnSb	-0.132	3.176	-0.098	0.011	2.956
RhMnSb	-0.134	3.565	-0.144	<0.001	3.287
IrMnSb	-0.192	3.332	-0.114	-0.003	3.022
FeMnSb	-0.702	2.715	-0.053	0.019	1.979

tion here that IrMnSb is in reality crystallizing in the $Ir_{0.92}Mn_{1.16}Sb_{0.92}$ stoichiometry.[2] The remaining compounds are known to exhibit a small disorder,[2] with the exception of CoMnSb.[38] Kaczmarska *et al.* have calculated using the KKR method within the coherent potential approximation the spin magnetic moments for a $(Co_{0.5}Mn_{0.5})_2Sb$ system, where the Co and Mn sites are completely disordered, and found them to agree with the experimental values.[39] In Fig. 2 we present the spin-projected total density of states (DOS) for all the six compounds. We remark that all six compounds present a gap, which is more wide in the compounds containing Co, Rh or Ir than Ni, Pd or Pt. Sb p states occupy the lowest part of the DOS shown in the figure, while the Sb s states are located ∼12 eV below the Fermi level. For the Ni compound the Fermi level is at the middle of the gap and for PtMnSb at the left edge of the gap in agreement with previous full-potential linear muffin-tin orbitals method (FPLMTO) calculations on these compounds.[22] The gap in the minority NiMnSb band is about 0.5 eV wide in good agreement with the experiment of Kirillova and collaborators[15] who analyzing their infrared spectra estimated a gap width of ∼0.4 eV. In the case of CoMnSb the gap is considerably larger (∼1 eV) than in the previous two compounds and the Fermi level is located at the left edge of the spin-down gap. CoMnSb has been studied theoretically by Kübler using the augmented spherical waves (ASW) method. He found a DOS similar to ours, with a large gap of comparable width and the Fermi level was also located at the left edge of the spin-minority gap.[40] For the other three compounds the Fermi level is located below the gap, although in the case of PdMnSb and IrMnSb it is very near to the edge of the gap.

The DOS of the different systems are mainly characterized by the large exchange-splitting of the Mn d states which is around 3 eV in all cases. This is clearly seen in the atom-projected DOS of NiMnSb in Fig. 4. This large exchange splitting leads to large localized spin moments at the Mn site; the existence of the localized moments has been verified also experimentally.[41] The localization comes from the fact that although d electrons of Mn are itinerant, the spin-down electrons are almost excluded from the Mn site. In Table I we present the spin magnetic moments at the different sites for all the compounds under study. Here we should mention that in order to calculate the moments we integrate the spin-projected charge density inside every Wigner-Seitz polyhedron. In our calculations these polyhedra were the same for every atom in the $C1_b$ structure. Mn moments approach in the case of the Ni, Pd and Pt compounds the 4 μ_B and they agree perfectly with previous FPLMTO calculations.[22] Ni, Pd and Pt are ferromagnetically coupled to Mn with small induced magnetic moments, while in all cases the Sb atom is antiferromagnetically coupled to Mn. Overall the calculated moments for the Ni, Pd and Pt compounds are in very good agreement with previous *ab-initio* results.[22,23] Experimental values for the spin-moment at the Mn site can be deduced from the experiments of Kimura *et al.*[42] by applying the sum rules to their x-ray magnetic circular dichroism spectra and the extracted moments agree nicely with our results; they found a Mn spin moment of 3.85 μ_B for NiMnSb, 3.95 μ_B for PdMnSb and 4.02 μ_B for PtMnSb. In the case of the Co-, Rh-, and IrMnSb compounds the spin magnetic moment of the X atom is antiparallel to the Mn localized moment and the Mn moment is generally about 0.5 μ_B smaller than in the Ni, Pd and Pt compounds. The Sb atom is here again antiferromagnetically coupled to the Mn atom.

The total magnetic moment in μ_B is just the difference between the number of spin-up occupied states and the spin-down occupied states. In the half-ferromagnetic compounds all spin-down states of the valence band are occupied and thus their total number should be, as in a semiconductor, an integer and the total magnetic moment should be also an integer since the total valence charge is an integer. A detailed discussion of the relation between the total moment and the number of electrons will be given in Section V. Here we notice only that the local moment per unit cell as given in Table I is close to 4 μ_B in the case of NiMnSb, PdMnSb and PtMnSb,

TABLE II: Number of electrons, n_{e^-}, lost (-) or gained (+) by an atom with respect to the free atom. As was the case for the spin moments the total number of electrons is calculated by integrating the total charge density inside a polyhedron.

n_{e^-}	X	Mn	Sb	Void
NiMnSb	+0.567	-0.456	-1.429	+1.318
PdMnSb	+0.237	-0.343	-1.080	+1.186
PtMnSb	+0.034	-0.212	-1.041	+1.219
CoMnSb	+0.516	-0.411	-1.426	+1.321
RhMnSb	+0.150	-0.273	-1.112	+1.235
IrMnSb	-0.074	-0.145	-1.031	+1.250

which is in agreement with the half-ferromagnetic character (or nearly half-ferromagnetic character in the case of PdMnSb) observed in Fig. 2. Note that due to problems with the ℓ_{max} cutoff the KKR method can only give the correct integer number 4, if Lloyd's formula has been used in the evaluation of the integrated density of states, which is not the case in the present calculations. We also find that the local moment of Mn is not far away from the 4 μ_B although there are significant (positive) contributions from the X-atoms and negative contribution from the Sb atom. In contrast to this we find that for the half-metallic CoMnSb and IrMnSb compounds the total moment is about 3 μ_B. Also the local moment of Mn is reduced, but only by about 0.5 μ_B. The reduction of the total moment to 3 μ_B is therefore accompanied by negative Co and Ir spin moments, *i.e* these atoms couple antiferromagnetically to the Mn moments. The reason for this behavior can be understood from the spin-polarized DOS of NiMnSb and CoMnSb shown in Fig. 3 (middle panel). The hybridization between Co and Mn is considerably larger than between Ni and Mn. Therefore the minority valence band of CoMnSb has a larger Mn admixture than the one of NiMnSb whereas the minority conduction band of CoMnSb has a larger Co admixture than the Ni admixture in the NiMnSb conduction band, while the populations of the majority bands are barely changed. As a consequence, the Mn moment is reduced by the increasing hybridization, while the Co moment becomes negative, resulting finally in a reduction of the total moment from 4 to 3 μ_B. Here we should note that further substitution of Fe for Co leads also to a half-ferromagnetic alloy with a total spin magnetic moment of 2 μ_B as has been already shown by de Groot *et al.* in Ref. 43 and shown by our calculations in Table I. The hybridization in the minority band between the Fe and Mn d-states is even larger than between the Co and Mn atoms in the CoMnSb compound, resulting in a further decrease of the Mn moment to around 2.7 μ_B and a larger negative moment at the Fe site (around -0.7 μ_B) compared to the Co site, which stabilize the half-ferromagnetic phase. Finally, in the case of RhMnSb the Fermi level is considerably below the gap and thus a part of the spin-down states are unoccupied leading to a total spin magnetic moment larger than the 3 μ_B of CoMnSb and IrMnSb.

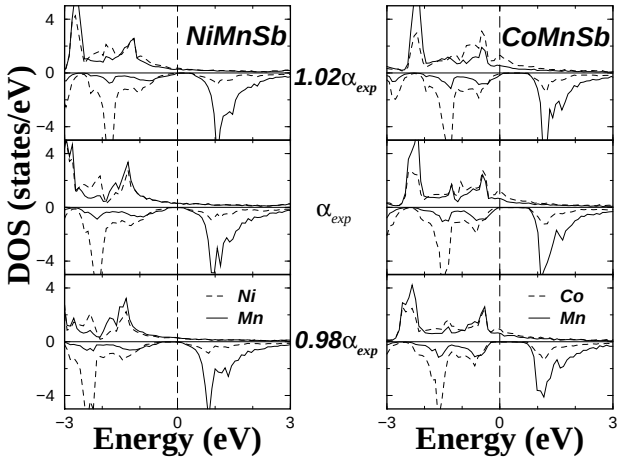

FIG. 3: Atomic- and spin-projected DOS of NiMnSb and CoMnSb when we contract (bottom panel) or expand (upper panel) the experimental lattice parameter by 2%.

It is also interesting to study the charge transfer in these compounds. In Table II we have gathered the number of electrons gained (+) or lost(-) by each atom in the different compounds with respect to the atomic total charge. To calculate them we simply integrated the total charge density inside each Wigner-Seitz polyhedron. It is obvious that the trends in this case are not like in the magnetic moments, where we found a similar behavior for isoelectronic systems. Since the d valence wavefuctions would have about the same spatial extent for neighboring elements in the same row, we expect a similar behavior for compounds containing an X atom in the same row of the periodic table. In the case of NiMnSb and CoMnSb we have the largest charge transfer, Ni and Co atoms gain $\sim 0.5e^-$ and Mn and Sb atoms lose around $0.4e^-$ and $1.4e^-$, respectively (results are similar for FeMnSb). Since the $3d$ wave functions are less extended than the $4d$ and $5d$, the atom-projected charge should be larger for Ni and Co than for the other transition metal atoms; Pd and Rh gain only $\sim 0.2e^-$ and for Pt and Ir the charge transfer is very small. In all the compounds under study the vacant site is found to contain a little bit more than one electron.

IV. EFFECT OF THE LATTICE PARAMETER

In this Section we will study the influence of the lattice parameter on the electronic and magnetic properties of the $C1_b$ Heusler alloys. Before starting this discussion we should mention that the generalized gradient approximation (GGA)[44] as expected gives better results than LDA concerning the equilibrium lattice parameters and as it has been already shown[22] GGA equilibrium lattice parameter differs only slightly from the experimental lattice constant. Moreover our tests showed that for the

TABLE III: Spin magnetic moments in μ_B for NiMnSb and CoMnSb when we contract or expand the experimental lattice parameter by 2%.

$m^{\rm spin}(\mu_B)$	a (a_{exp})	Ni or Co	Mn	Sb	Void	Total
NiMnSb	0.98	0.314	3.625	-0.042	0.063	3.960
	1.00	0.264	3.705	-0.060	0.052	3.960
	1.02	0.199	3.795	-0.085	0.043	3.952
CoMnSb	0.98	0.037	3.002	-0.090	0.012	2.960
	1.00	-0.132	3.176	-0.098	0.011	2.956
	1.02	-0.305	3.371	-0.102	0.013	2.976

same lattice parameter LDA and GGA give exactly the same results for the gap and the position of the Fermi level with respect to it, although they produce slightly different spin magnetic moments. So the use of LDA and of the experimental lattice parameter should be considered enough to accurately describe the experimental situation. In Fig. 3 we have plotted the DOS for CoMnSb and NiMnSb when we contract and expand the lattice parameter by 2% with respect to the experimental lattice constant. Either expansion or contraction results in a practically rigid shift of the bands with small rearrangements of the shape of the peaks to account for charge neutrality. Expansion moves the Fermi level deeper in energy, *i.e.* closer to the minority occupied states, while contraction moves the Fermi level higher in energy. Especially in the case of PdMnSb and IrMnSb, where the Fermi level was near the left edge of the gap, a contraction by 2% is enough to move the Fermi level inside the gap, as it was already shown in the case of PdMnSb.[22] This can be easily understood in terms of the behavior of the p electrons of the Sb atom. When we make a contraction then we squeeze mainly the delocalized p electrons of Sb, as the d electrons of the transition metal atoms are already well localized. So the Sb p states move higher in energy compared to the d electrons of the transition metal and the Mn atom and due to charge neutrality also the Fermi level moves higher in energy compared to the experimental lattice constant case. Expansion has the opposite effect.

Also the magnetic moments change with the lattice parameter and in Table III we have gathered, for the cases shown in Fig. 3, the spin magnetic moments. As will be discussed below the total magnetic moment does not change and remains close to 4 μ_B for NiMnSb and to 3 μ_B for CoMnSb, as in all cases the Fermi level falls inside the gap and the number of spin-down occupied states does not change; even in CoMnSb, when we contract by 2%, the Fermi level is just below the left edge of the gap. When we expand NiMnSb the Ni spin moment decreases, while the Mn spin moment increases. Expansion and contraction change the atom-projected charges by less than 0.01 electron with respect to the experimental lattice constant. Thus any moment changes are accompanied by changes of equal magnitude, but opposite sign in the population of the local majority and minority states.

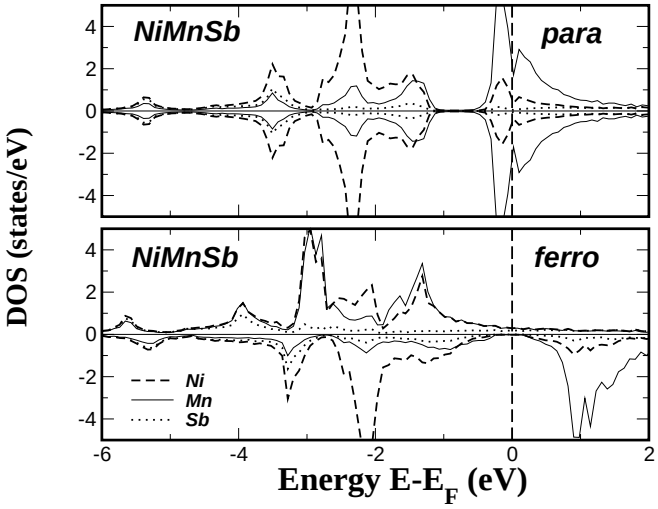

FIG. 4: Ferro- and para-magnetic atomic- and spin-resolved density of states of NiMnSb. Note that the bonding d states are mainly of Ni character, while the antibonding d states are mainly of Mn character, and they are separated by a gap.

When the lattice is expanded, the Mn goes towards a more atomiclike situation and its magnetic moment increases while the hybridization with the Ni d states decreases. The opposite situation occurs when we contract NiMnSb; Mn moment decreases, hybridization with Ni d states increases and so does the Ni spin magnetic moment. A similar trend is observed for CoMnSb. The Mn moments increases with expansion and decreases with contraction, while the Co moment, coupling antiparallel to Mn in the unexpanded lattice, decreases on expansion to larger negative values and increases on contraction to slightly positive values. So finally the lattice parameter has a significant effect on the magnetic properties of the Heusler alloys, with the local moments changing substantially, but the total moment and the local charges being stable.

V. ORIGIN OF THE GAP

The gap basically arises from the covalent hybridization between the lower-energy d states of the high-valent transition metal (TM) atom like Ni or Co and the higher-energy d states of the lower-valent TM atom, leading to the formation of bonding and antibonding bands with a gap in between. The bonding hybrids are localized mainly at the high-valent TM atom site while the unoccupied antibonding states mainly at the lower-valent TM atom site. For instance in Fig. 4 the minority occupied bonding d states are mainly of Ni character while the unoccupied antibonding states are mainly of Mn character. Similarly to the situation of the elemental and compound semiconductors, these structures are particularly stable when only the bonding states are occupied. In binary TM alloys this situation usually does not occur, since

the total charge is too large to be accommodated in the bonding hybrids only, or, if this is possible, the covalent hybridization is not sufficient to form a gap, at least not for the close-packed structures of the transition metal alloys (see below).

For these reasons the *sp*-elements like Sb play an important role for the existence of the Heusler alloys with a gap at the E_F. While an Sb atom has 5 valence electrons ($5s^2$, $5p^3$), in the NiMnSb compound each Sb atom introduces a deep lying *s*-band, at about -12 eV, and three *p*-bands being pushed by hybridization below the center of the *d*-bands. These *s*- and *p*-bands accommodate a total of 8 electrons per unit cell, so that formally Sb acts as a triple charged Sb^{-3} ion. Analogously, a Te-atom behaves in these compounds as a Te^{-2} ion and a Sn-atom as a Sn^{-4} ion. This does not mean, that locally such a large charge transfer exists. In fact, the *p*-states strongly hybridize with the TM *d*-states and the charge in these bands is delocalized. Table II shows that locally Sb even looses about one electron. What counts is, that the *s*- and *p*-bands accommodate 8 electrons per unit cell, thus effectively reducing the *d*-charge of the TM atoms. Since the bonding *d*-bands introduced above can accommodate 10 electrons, one expects therefore that the non-magnetic Heusler alloy with 18 valence electrons per unit cell are particularly stable and have a gap at E_F, i.e. are semiconducting, which requires, of course, a sufficient strong covalency between the TM partners for the gap to exist. This "18-electron rule" was recently derived by Jung *et al.* based on ionic arguments.[45] Examples for the semiconducting $C1_b$ Heusler alloys are CoTiSb and NiTiSn.[46] In the case of CoTiSb the Sb atom brings 5 valence electrons and the Co and Ti atoms 9 and 4, respectively. Of the 13 TM electrons 3 are catched by the Sb atom, so that the remaining 10 electrons just fill the bonding *d*-bands. In the case of NiTiSn, the Ni atom brings in one more electron than Co, but the Sn atom with 4 valence electrons catches away in addition 4 *d*-electrons, so that again 10 electrons remain for the bonding *d* bands.

Also for systems with more (or less) than 18 electrons, the gap can still exist. These systems are no longer semiconducting and loose part of the stability, since then also anti-bonding states are occupied (or not all bonding states are occupied). An example is the paramagnetic DOS of NiMnSb, shown in Fig. 4. Of the 22 valence electrons, four have to be accommodated in the antibonding *d*-bands. The high DOS at E_F signalizes that the Stoner criterium is met so that in $C1_b$ structure NiMnSb should be a ferromagnet. Of the possible magnetic states, the half-metallic states, as shown by the spin polarized DOS of NiMnSb in Fig. 4, is particularly favored due to the gap at E_F in the minority band. Thus for these half-metallic Heusler alloys the 18-electron rule for the semiconducting Heusler is replaced by a 9-electron rule for the number of minority electrons. By denoting the total number of valence electrons by Z_t, being an integer itself, the total moment M_t per unit cell is then given by the simple rule $M_t = Z_t - 18$ in μ_B, since $Z_t - 18$ gives the number of

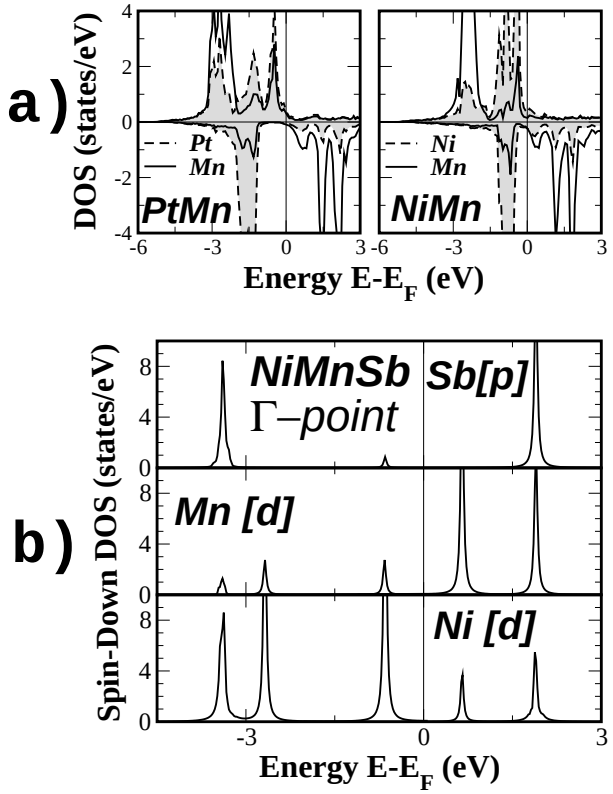

FIG. 5: *a*) Atom- and spin-projected DOS for PtMn and NiMn using the lattice constants of PtMnSb and NiMnSb respectively. The Sb atom has been substituted with a vacant site. *b*) Atom- and orbital-projected spin-down DOS of NiMnSb projected at the Γ point. We have used a small broadening to calculate the DOS.

uncompensated spins. Thus the total moment M_t is an integer quantity, assuming the values 0, 1, 2, 3, 4 and 5 if $Z_t \geq 18$. The value 0 corresponds to the semiconducting phase and the value 5 to the maximal moment when all 10 majority *d*-states are filled.

Our explanation differs from the one of de Groot and his collaborators in the pioneering paper of 1983.[5] There, the gap has been discussed in terms of the interaction between the Mn and Sb atoms, and the Ni atom has been completely omitted from the discussion. But Mn and Sb are second-neighbors and their hybridization is much weaker than between the Mn and Ni atoms which are first-neighbors which clearly shows up in Fig. 4. Furthermore the states at the edges of the gap are of Mn and Ni character, and Sb has a very small weight contrary to the explanation of de Groot *et al.* that proposed that the states just below the gap are of Sb character. To further demonstrate the importance of the *d*-*d* hybridization for the gap, we have performed ground state calculations for NiMn in the zinc-blende structure, *i.e.* by replacing the Sb atom in the $C1_b$ structure of NiMnSb by a vacant site, but using the lattice parameter of NiMnSb. The calculations, as shown in Fig. 5a, yield a pseudogap in the minority gap at E_F. For the hypothetical isoelec-

tronic compound PtMn, the analogous calculation yields by using the lattice constant of PtMnSb, a real gap at E_F. In this case the minority valence band consists of a low-lying s-band and 5 bonding d-bands of mostly Pt character, while the minority conduction band is formed by 5 antibonding d-bands of mostly Mn character. Thus the rule for the total moments, $M_t = Z_t - 18$, is for this alloy replaced by $M_t = Z_t - 12$, due to the six minority valence bands. For PtMn this yields M_t=17-12=5μ_B, which is indeed obtained in the calculations. Thus the Sb atom is not necessary for the formation of the gap (but plays a crucial role to stabilize these materials as TM alloys like PtMn or NiMn do not favor such an open structure).

To further elucidate the difference between our interpretation and the one in Ref. 5 we have drawn in the lower panel of Fig. 5 the site projected DOS of NiMnSb for the bands at the Γ point; we have used a small imaginary part of the energy to better see the size of the contributions from different sites. Note here that the character of the wavefunctions at the Γ-point coincides with the character of the real space wavefunctions. The three panels show the contribution of the Sb p-states, Ni d-states and Mn d-states to the bands at Γ. We do not present the full band structure since it is similar to the one already presented in Ref. 5. There is a band very low in energy, around 12 eV below the Fermi level, which is provided by the s electrons of Sb (not shown in the figure). The next triple degenerated band at ~ 3.5 eV below the Fermi level is originating from the p electrons of Sb and has a strong admixture of Ni d states. As we have already mentioned the p states of Sb couple strongly to d TM states and more precisely to the t_{2g} hybrids which transform following the same representation in the case of the tetrahedral symmetry T_d. Through this mechanism this band created mainly by the p electrons of Sb accommodates also transition metal d electrons reducing the effective d charge that can be therefore accommodated in the higher bands. Just above this band we find the double degenerated band created by the e_g electrons of the transition metal atoms. Finally, the triple degenerated band just below the Fermi level is created by the bonding t_{2g} states of Ni and Mn with a tiny admixture of Sb p electrons. Above the band gap we find the antibonding double degenerated e_g TM states and the triple degenerated t_{2g} states. The band created by the latter ones has a strong admixture of Sb-p states. This admixture of Sb p-states to the Mn-dominated t_{2g} band is sizeable. However it occurs only at the Γ point. When averaged over the full-Brillouin zone, the Sb-admixture in the conduction band is tiny as can be seen in Fig. 4.

Thus our explanation of the valence and conduction bands is internally consistent. It explains the existence of exactly 9 minority valence bands and simultaneously describes the magnetic properties of these compounds. With small modifications it can be also extended to explain the properties of the half-ferromagnetic full-Heusler alloys like Co_2MnGe.[47] Nevertheless the Sb atoms or in general the sp atoms are important for the properties of the Heusler alloys. Firstly they stabilize the $C1_b$ structure, being very unusual for transition metal compounds. Secondly they provide the four low-lying s- and p-bands, which can be filled with additional d-states. Thus by varying the valence of the sp atoms, the total moments follow the rule $M_t = Z_t - 18$ describing a rich variety of possible magnetic properties.

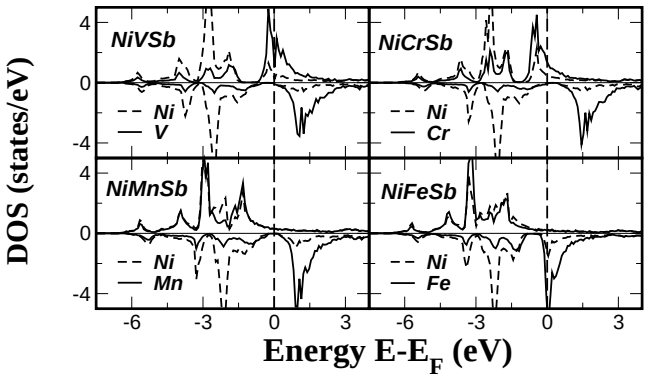

FIG. 6: Calculated atom- and spin-projected density of states of NiYSb, with Y= V, Cr, Mn and Fe using the lattice parameter of NiMnSb. Notice that in the case of the V and Cr compounds also the spin-up band has a gap.

Here we want also to point to the similarities of the above moment behavior to the well-known Slater-Pauling curve for the TM alloys.[40] The difference is, that in the Heusler alloys the TM minority population is fixed at 5 and the screening is achieved by filling the majority band, while in the binary TM alloys the majority band is filled and the charge neutrality is achieved by filling the minority states. As a result, for the Heusler alloys the moment increases with the total charge Z_t, while in the TM binary alloys it decreases with increasing Z_t, since the total moment is given by $M_t \simeq 10 - Z_t$.

VI. SLATER-PAULING CURVE AND THE ROLE OF THE LOWER-VALENT TRANSITION METAL ATOM

As we mentioned in the last paragraph above the half-ferromagnetic Heusler alloys follow the Slater-Pauling curve at least when we change the higher-valent transition element (substituting Co or Fe for Ni). Here we want to study this behavior, when we vary the valence of the lower-valent (*i.e.* magnetic) transition metal atom. Thus we substitute V, Cr and Fe for Mn in the NiMnSb and CoMnSb compounds using the experimental lattice constants of the two Mn compounds. Only NiVSb and CoVSb exist experimentally. NiVSb crystallizes in a Ni_2In hexagonal structure.[48] KKR calculations by Tobola and Pierre show that this is energetically the most favorable structure due to the fact the Fermi level falls inside a peak of the spin-up states.[4] On the other

TABLE IV: Spin magnetic moments in μ_B for the NiYSb and CoYSb compounds where Y stands for V, Cr, Mn and Fe. For all the calculations we have used the experimental lattice constants of the NiMnSb and CoMnSb alloys.

$m^{\rm spin}(\mu_B)$	Ni or Co	Y	*sp* atom	Void	Total
NiVSb	0.139	1.769	-0.040	0.073	1.941
NiCrSb	0.059	2.971	-0.113	0.059	2.976
NiMnSb	0.264	3.705	-0.060	0.052	3.960
NiFeSb	0.404	2.985	-0.010	0.030	3.429
CoVSb	-0.126	1.074	-0.021	0.038	0.965
CoCrSb	-0.324	2.335	-0.077	0.032	1.967
CoMnSb	-0.132	3.176	-0.098	0.011	2.956
CoFeSb	0.927	2.919	-0.039	0.012	3.819

hand CoVSb crystallizes in the $C1_b$ structure presented in Fig. 1 and it has been studied using first-principle calculations by Tobola *et al.*[46] who have shown that it is also a half-ferromagnetic material with a total spin moment of 1 μ_B. Its experimental lattice constant of 5.801Å^2 is very close to the one of CoMnSb (5.853Å) and our results are similar for both of them.

In Table IV we present the spin magnetic moments for all these compounds and in Fig. 6 the calculated total DOS for the NiYSb alloys assuming that all these compounds are ferromagnetic (results are similar for the CoYSb compounds). The compounds containing V and Cr are also half-ferromagnetic as NiMnSb and CoMnSb. As can be seen in Table IV when we substitute Cr for Mn we mainly depopulate one spin-up *d* state of the lower-valent transition metal atom and thus the spin magnetic moment of this atom is reduced practically by 1 μ_B. A similar phenomenon occurs when we substitute V for Cr. This behavior is reflected in the smaller exchange-splitting of the V and Cr *d* bands compared to the Mn bands as can be seen in Fig. 6. These compounds keep the half-ferromagnetic character of NiMnSb and CoMnSb and therefore their total spin magnetic moments follow the Slater-Pauling curve imposed by the "9-electron minority gap" rule. The compound with 22 valence electrons (NiMnSb) has a total spin moment of 4 μ_B, the compounds with 21 valence electrons (NiCrSb and CoMnSb) 3 μ_B, the compounds with 20 valence electrons (NiVSb and CoCrSb) 2 μ_B and finally CoVSb that has only 19 electrons has a total spin moment of 1 μ_B. Here we should remind that CoTiSb, an 18-electrons system, is a semiconductor.

As a last test we have substituted Fe for Mn in CoMnSb and NiMnSb, but both CoFeSb and NiFeSb loose their half-ferromagnetic character. In the case of NiFeSb the majority *d*-states are already fully occupied as in NiMnSb, thus the additional electron has to be screened by the minority *d*-states, so that the Fermi level falls into the minority Fe states and the half-metallicity is lost; for half-metallicity a total moment of 5 μ_B would be required which is clearly not possible. For CoFeSb the situation is more delicate. This system has 22 valence electrons and if it would be a half-ferromagnet it should have a total spin-moment of 4 μ_B like NiMnSb. In reality our calculations indicate that the Fermi level is slightly above the gap and the total spin-moment is slightly smaller than 4 μ_B. The Fe atom possesses a comparable spin-moment in both NiFeSb and CoFeSb compounds contrary to the behavior of the V, Cr and Mn atoms. Furthermore, contrary to the other Co compounds presented in Table IV in the case of CoFeSb the Co and the lower-valent TM atom (Fe) are ferromagnetically coupled.

TABLE V: Spin magnetic moments in μ_B for the NiMnZ compounds where Z stands for a *sp* atom belonging at the 5th row of the periodic table .

$m^{\rm spin}(\mu_B)$	Ni	Mn	*sp* atom	Void	Total
NiMnIn	0.192	3.602	-0.094	0.003	3.704
NiMnSn	0.047	3.361	-0.148	-0.004	3.256
NiMnSb	0.264	3.705	-0.060	0.052	3.960
NiMnTe	0.467	3.996	0.101	0.091	4.656

VII. ROLE OF THE *sp* ATOM

In this Section we will continue our study on the role of the *sp* atom in the electronic properties of a $C1_b$ compound. We performed calculations using the same lattice parameter as with NiMnSb but substituting Sb by another *sp* atom in the periodic table and in Fig. 7 we present the obtained spin-projected DOS. For the presentation we ordered them following the position of the *sp* atom in the periodic table. Firstly we will discuss the trend along a row in the periodic table and more precisely the substitution of Sb by In and Sn that have one and two less valence electrons, respectively, and Te that has one electron more than Sb. It is obvious looking at Fig. 7 than the substitution of In, Sn or Te for Sb changes the number of valence electrons and the position of the Fermi level with respect to the gap to account for this extra or missing *p* electrons. So for Te the Fermi level is above the spin-down gap while for Sn it is below the gap and for In it is even lower than Sn. The change of the position of the Fermi level is accompanied by changes in the shape of the peaks to account for charge neutrality. The same trend can be found along all the other rows presented in this figure. Thus the change of the valence of the *sp* atom does not preserve the half-ferromagnetic character of NiMnSb, but rather leads to a shift of the Fermi level analogous to a rigid band model. The only exception from this rule is NiMnSe, which is nearly half-metallic. Here we see big changes in the majority band, where antibonding *p*-*d* states, which are usually above E_F, are shifted below the Fermi level, thus increasing the total moment to 4.86 μ_B, *i.e.* to nearly 5 μ_B.

More interesting is the substitution of Sb by an isoelectronic atom. Substituting Bi for Sb produces a similar DOS with the Fermi level being at the middle of the gap

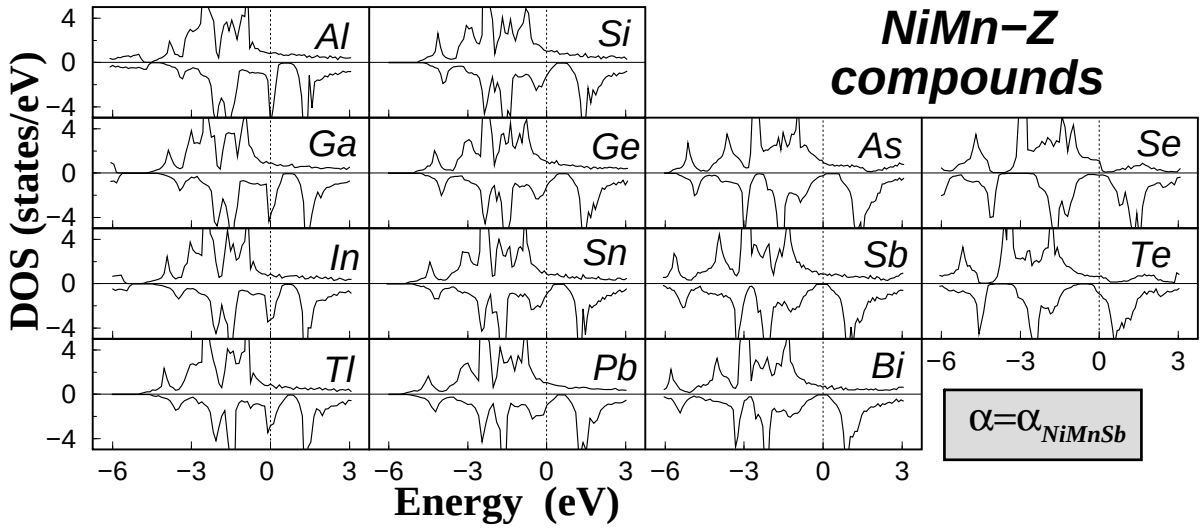

FIG. 7: Spin-resolved density of states of NiMnSb and when substituting Sb by another *sp* atom. All calculations have been performed using the experimental lattice constant of NiMnSb.

as for NiMnSb. If now we substitute As for Sb then the Fermi level moves and now it is found at the left edge of the gap. In the case of NiMnSb and NiMnBi the majority p states of Sb(Bi) hybridize stronger with the d states of the TM atoms and thus they extent higher in energy compared to the p states of As in NiMnAs. As a result the Fermi level is deeper in energy in the case of the As-compound. Presumably for the correct lattice constant of NiMnAs, being somewhat smaller than the one of NiMnSb used in the calculation, the Fermi energy would move again into the gap.

The spin moments are similar for compounds containing *sp* atoms in the same column. For example Ni spin magnetic moment is around $\sim$0.2 μ_B for the Al, Ga, In and Tl based compounds , practically zero for the Si, Ge, Sn and Pb compounds, it increases again to $\sim$0.2-0.3 μ_B for the As, Sb and Bi compounds and it reaches $\sim$0.5 μ_B for the Se and Te compounds. In Table V we present the spin magnetic moments for compounds containing In, Sn, Sb and Te to give an estimation of the spin moments in the other compounds. Of course we should keep in mind that all these calculations have been performed at the NiMnSb experimental lattice constant and the position of the Fermi level would change at the real lattice parameters.[49] But to our knowledge none of this compounds has been yet studied experimentally with the exception of NiMnAs which was found to crystallize in the hexagonal Fe_2P structure,[50] but modern techniques like molecular beam epitaxy may enable its growth in the $C1_b$ structure.

In conclusion substituting the *sp* atom in NiMnSb destroys the half-metallicity. In a first approximation, the *sp*-elements act as acceptors and the Fermi level is shifted in a rigid band model.

VIII. CONCLUSION

In this contribution we have studied in detail the electronic properties of the half-ferromagnetic Heusler alloys and mainly focused on the appearance of the gap and the related magnetic properties. We have shown using the full-potential version of the screened KKR method that the gap in the $C1_b$ compounds is imposed by the lattice structure. As in the diamond and zinc-blende structures of the semiconductors, the hybridization splits both the spin-up and spin-down d bands. While systems with 18 valence electrons, like CoTiSb, are semiconductors, in the systems with a larger number of valence electrons also antibonding states are populated and the paramagnetic phase becomes unstable. The half-ferromagnetic phase is favorable as the system can gain energy when the Fermi level falls within the gap of the minority band. It is stabilized by the large exchange splitting of the lower-valent transition metal atom and by the *sp* atom which creates one s and three p bands lying low in energy and which accommodate transition metals valence electrons. The minority occupied bands accommodate a total of nine electrons (the minority bonding transition-metal d states accommodate 5 electrons) and the total magnetic moment in μ_B is just the difference between the total number of valence electrons and 2×9. As a result of this simple rule for the total magnetic moment the half-ferromagnetic Heusler compounds follow the Slater-Pauling curve. We have verified this behavior in the case of the NiYSb and CoYSb compounds where Y accounts for V, Cr and Mn. In the case of NiFeSb also minority antibonding states are populated and the half-ferromagnetic character is lost. Changing the lattice parameter results in shifting the Fermi level without destroying the gap. The majority states of the *sp* atom

atom play also an important role as the extent of the p states through their hybridization with the d states determines the position of the Fermi level with respect to the gap. Changing the sp atom results in a practically rigid shift of the bands destroying the half-metallicity.

Acknowledgments

The authors acknowledge financial support from the RT Network of *Computational Magnetoelectronics* (contract RTN1-1999-00145) of the European Commission.

* Electronic address: I.Galanakis@fz-juelich.de

[1] F. Heusler, Verh. Dtsch. Phys. Ges. **5**, 219 (1903).

[2] P. J. Webster and K. R. A. Ziebeck, in *Alloys and Compounds of d-Elements with Main Group Elements. Part 2.*, edited by H. R. J. Wijn, Landolt-Boörnstein, New Series, Group III, Vol. 19,Pt.c (Springer-Verlag, Berlin), pp. 75-184.

[3] J. Pierre, R. V. Skolozdra, J. Tobola, S. Kaprzyk, C. Hordequin, M. A. Kouacou, I. Karla, R. Currat, and E. Lelièvre-Berna, J. Alloys Comp. **262-263**, 101 (1997).

[4] J. Tobola and J. Pierre, J. Alloys Comp. **296**, 243 (2000).

[5] R. A. de Groot. F. M. Mueller, P. G. van Engen, and K. H. J. Buschow, Phys. Rev. Lett. **50**, 2024 (1983).

[6] S. A. Wolf, D. D. Awschalom, R. A. Buhrman, J. M. Daughton, S. von Molnár, M. L. Roukes, A. Y. Chtchelkanova, and D. M. Treger, Science **294**, 1488 (2001); G. A. Prinz, Science **282**, 1660 (1998); G. A. Prinz, J. Magn. Magn. Mater. **200**, 57 (1999).

[7] R. J. Soulen Jr., J. M. Byers, M. S. Osofsky, B. Nadgorny, T. Ambrose, S. F. Cheng, P. R. Broussard, C. T. Tanaka, J. Nowak, J. S. Moodera, A. Barry, and J. M. D. Coey, Science **282**, 85 (1998).

[8] H. Akai, Phys. Rev. Lett. **81**, 3002 (1998).

[9] H. Akinaga, T. Manago, and M. Shirai, Jpn. J. Appl. Phys. **39**, L1118 (2000); I. Galanakis, Phys. Rev. B **66**, 012406 (2002).

[10] J.-H. Park, E. Vescovo, H.-J. Kim, C. Kwon, R. Ramesh, and T. Venkatesan, Nature **392**, 794 (1998).

[11] S. Datta and B. Das, Appl. Phys. Lett. **56**, 665 (1990).

[12] K. A. Kilian and R. H. Victora, J. Appl. Phys. **87**, 7064 (2000).

[13] C. T. Tanaka, J. Nowak, and J. S. Moodera, J. Appl. Phys. **86**, 6239 (1999).

[14] J. A. Caballero, Y. D. Park, J. R. Childress, J. Bass, W.-C. Chiang, A. C. Reilly, W. P. Pratt Jr., and F. Petroff, J. Vac. Sci. Technol. A **16**, 1801 (1998); C. Hordequin, J. P. Nozières, and J. Pierre. J. Magn. Magn. Mater. **183**, 225 (1998).

[15] M. M. Kirillova, A. A. Makhnev, E. I. Shreder, V. P. Dyakina, and N. B. Gorina, Phys. Stat. Sol. (b) **187**, 231 (1995).

[16] K. E. H. M. Hanssen and P. E. Mijnarends, Phys. Rev. B **34**, 5009 (1986); K. E. H. M. Hanssen, P. E. Mijnarends, L. P. L. M. Rabou, and K. H. J. Buschow, Phys. Rev. B **42**, 1533 (1990).

[17] W. van Roy, J. de Boeck, B. Brijs, and G. Borghs, Appl. Phys. Lett. **77**, 4190 (2000); J.-P. Schlomka, M. Tolan, and W. Press, Appl. Phys. Lett. **76**, 2005 (2000).

[18] F. B. Mancoff, B. M. Clemens, E. J. Singley, and D. N. Basov, Phys. Rev. B **60**, *R*12 565 (1999).

[19] W. Zhu, B. Sinkovic, E. Vescovo, C. Tanaka, and J. S. Moodera, Phys. Rev. B **64**, *R*060403 (2001).

[20] D. Ristoiu, J. P. Nozières, C. N. Borca, T. Komesu, H.-K. Jeong, and P. A. Dowben, Europhys. Lett. **49**, 624 (2000); D. Ristoiu, J. P. Nozières, C. N. Borca, B. Borca, and P. A. Dowben, Appl. Phys. Lett. **76**, 2349 (2000); T. Komesu, C. N. Borca, H.-K. Jeong, P. A. Dowben, D.Ristoiu, J. P. Nozières, Sh. Stadler, and Y. U. Idzerda, Phys. Lett. A **273**, 245 (2000).

[21] C. Hordequin, D. Ristoiu, L. Ranno, and J. Pierre, Eur. Phys. J. B **16**, 287 (2000); C. N. Borca, T. Komesu, H.-K. Jeong, P. A. Dowben, D. Ristoiu, Ch. Hordequin, J. P. Nozières, J. Pierre, Sh. Stadler, and Y. U. Idzerda, Phys. Rev. B **64**, 052409 (2001).

[22] I. Galanakis, S. Ostanin, M. Alouani, H. Dreyssé, and J. M. Wills, Phys. Rev. B **61**, 4093 (2000).

[23] E. Kulatov and I. I. Mazin, J. Phys.: Condens. Matter **2**, 343 (1990); S. V. Halilov and E. T. Kulatov, J. Phys.: Condens. Matter **3**, 6363 (1991); X. Wang, V. P. Antropov, and B. N. Harmon, IEEE Trans. Magn. **30**, 4458 (1994). S. J. Youn and B. I. Min, Phys. Rev. B **51**, 10 436 (1995); V. N. Antonov, P. M. Oppeneer, A. N. Yaresko, A. Ya. Perlov, and T. Kraft, Phys. Rev. B **56**, 13 012 (1997).

[24] J. R. Reitz and M. B. Stearns, J. Appl. Phys. **50**, 2066 (1979).

[25] J. Kübler, A. R. Williams, and C. B. Sommers, Phys. Rev. B **28**, 1745 (1983).

[26] P. Larson, S. D. Mahanti, and M. G. Kanatzidis, Phys. Rev. B **62**, 12 574 (2000).

[27] D. Orgassa, H. Fujiwara, T. C. Schulthess, and W. H. Butler, Phys. Rev. B **60**, 13 237 (1999).

[28] G. A. Wijs and R. A. de Groot, Phys. Rev. B **64**, *R*020402 (2001).

[29] I. Galanakis, J. Phys.: Condens. Matt. **14**, 6329 (2002).

[30] S. J. Jenkins and D. A. King, Surf. Sci. **494**, L793 (2001).

[31] S. H. Vosko, L. Wilk, and N. Nusair, Can. J. Phys. **58**, 1200 (1980).

[32] P, Hohenberg and W. Kohn, Phys. Rev. **136**, B864 (1964); W. Kohn and L. J. Sham, Phys. Rev. **140**, A1133 (1965).

[33] R. Zeller, P. H. Dederichs, B. Újfalussy, L. Szunyogh, and P. Weinberger Phys. Rev. B **52**, 8807 (1995).

[34] N. Papanikolaou, R. Zeller, and P. H. Dederichs, J. Phys.: Condens. Matter **14**, 2799 (2002).

[35] R. Zeller, Phys. Rev. B **55**, 9400 (1997); K. Wildberger, R. Zeller, and P.H. Dederichs, Phys. Rev. B **55**, 10074 (1997).

[36] R. Zeller, J. Deutz, and P.H. Dederichs, Sol. St. Comm. **44**. 993 (1982); K. Wildberger, P. Lang, R. Zeller, and P.H. Dederichs, Phys. Rev. B **52**, 11502 (1995).
[37] H.J. Monkhorst and J.D. Pack, Phys. Rev. B **13**, 5188 (1976).
[38] M. J. Otto, R. A. M. van Woerden, P. J. van der Valk, J. Wijngaard, C. F. van Bruggen, C. Haas, and K. H. J. Buschow, J. Phys.: Condens. Matter **1**, 2341 (1989); M. J. Otto, R. A. M. van Woerden, P. J. van der Valk, J. Wijngaard, C. F. van Bruggen, and C. Haas, J. Phys.: Condens. Matter **1**, 2351 (1989).
[39] K. Kaczmarska, J. Pierre, J. Tobola, and R. V. Skolozdra, Phys. Rev. B **60**, 373 (1999).
[40] J. Kübler, Physica B **127**, 257 (1984).
[41] M. V. Yablonskikh, V. I. Grebennikov, Yu. M. Yarmoshenko, E. Z. Kurmaev, S. M. Butorin, L.-C. Duda, C. Såthe, T. Käämbre, M. Magnuson, J. Nordgren, S. Plogmann, and M. Neumann, Solid State Commun. **117**, 79 (2001); M. V. Yablonskikh, Yu. M. Yarmoshenko, V. I. Grebennikov, E. Z. Kurmaev, S. M. Butorin, L.-C. Duda, J. Nordgren, S. Plogmann, and M. Neumann, Phys. Rev. B **63**, 235117 (2001).
[42] A. Kimura, S. Suga, T. Shishidou, S. Imada, T. Muro, S. Y. Park, T. Miyahara, T. Kaneko, T. Kanomata, Phys. Rev. B **56**, 6021 (1997).
[43] R. A. de Groot, A. M. van der Kraan, and K. H. J. Buschow, J. Magn. Magn. Mater. **61**, 330 (1986).
[44] J.P. Perdew, K. Burke, and M. Ernzerhof, *Phys. Rev. Lett.* **77** (1996) 3865.
[45] D. Jung, H.-J. Koo, and M.-H. Whangbo, J. Mol. Struct. (Theochem) **527**, 113 (2000).
[46] J. Tobola, J. Pierre, S. Kaprzyk, R. V. Skolozdra, and M. A. Kouacou, J. Phys.: Condens. Matter **10**, 1013 (1998).
[47] I. Galanakis, P. H. Dederichs, and N. Papanikolaou, unpublished, preprint cond-mat/0205129.
[48] C. B. Evers, C. G. Richter, K. Hartjes, and W. Jeitschko, J. Alloys Comp. **252**, 93 (1997).
[49] D. E. Brandão, and A. A. Gomes, Phys. Stat. Sol. (a) **142**, 27 (1994).
[50] M. A. Nylund, A. Roger, J. P. Sénateur, and R. Fruchart, J. Solid State Chem. **4**, 115 (1972); T. Harada, T. Kanomata, and T. Kaneko, J. Magn. Magn. Mater. **90&91**, 169 (1990).